

This is the accepted manuscript made available via CHORUS. The article has been published as:

Chirality Switching and Winding or Unwinding of the Antiferromagnetic NiO Domain Walls in Fe/NiO/Fe/CoO/Ag(001)

J. Li, A. Tan, S. Ma, R. F. Yang, E. Arenholz, C. Hwang, and Z. Q. Qiu

Phys. Rev. Lett. **113**, 147207 — Published 3 October 2014

DOI: [10.1103/PhysRevLett.113.147207](https://doi.org/10.1103/PhysRevLett.113.147207)

Chirality switching and winding/unwinding of antiferromagnetic NiO domain walls in Fe/NiO/Fe/CoO/Ag(001)

J. Li,¹ A. Tan,¹ S. Ma,^{1,2} R. F. Yang,¹ E. Arenholz,³ C. Hwang,⁴ and Z. Q. Qiu¹

¹ *Department of Physics, University of California at Berkeley, Berkeley, California 94720, USA*

² *Shenyang National Laboratory for Materials Science, Institute of Metal Research, Chinese Academy of Sciences, Shenyang 110016, China*

³ *Advanced Light Source, Lawrence Berkeley National Laboratory, Berkeley, California 94720, USA*

⁴ *Korea Research Institute of Standards and Science, Yuseong, Daejeon 305-340, Korea*

Abstract

Fe/NiO/Fe/CoO/Ag(001) single crystalline films were grown epitaxially and investigated by X-ray Magnetic Circular Dichroism (XMCD) and X-ray Magnetic Linear Dichroism (XMLD). The bottom Fe layer magnetization is pinned through exchange coupling to the CoO layer and the top Fe layer magnetization can be rotated by an in-plane external magnetic field. We find that the NiO spins wind up to form a domain wall due to the perpendicular NiO/Fe interfacial coupling as the top layer Fe magnetization rotates from 0° to 90° , but switch wall chirality and unwind the wall as the Fe magnetization rotates from 90° to 180° . This observation shows that Mauri's 180° domain wall does not exist in perpendicularly coupled FM/AFM system in the strong coupling regime.

PACS numbers: 75.70.Ak

Exchange bias [1] refers to the shift of the magnetic hysteresis loop from zero magnetic field in a ferromagnet(FM)/antiferromagnet(AFM) system after field cooling to below the Néel temperature. Although it is widely used in magnetic recording technology, the mechanism of exchange bias has never been clearly resolved in the past five decades [2]. Early explanations assumed a perfectly uncompensated AFM interface which is magnetically coupled to the FM magnetization and the exchange bias is simply given by the FM/AFM interfacial coupling [3]. It was soon realized that this model is over simplified because it yields an exchange bias several orders of magnitude greater than the experimental values. This contradiction was addressed by assuming a mixed compensated/uncompensated AFM interface (e.g., by interfacial roughness) so that the residual overall interfacial coupling and the corresponding exchange bias should be significantly reduced [4]. However, this model depends heavily on the interfacial spin configurations, contradicting the relatively robust value of exchange bias found in experiments. Moreover, Koon showed that perpendicular FM/AFM interfacial magnetic coupling should be present even for a perfectly compensated AFM interface [5] though this coupling might not be responsible for exchange bias [6]. Further studies on FM/AFM interfacial coupling are more or less model dependent and aim to address specific AFM spin configurations to generating the exchange bias [7,8,9].

Different from the above approach which focuses on the interfacial FM/AFM coupling, Mauri et al. considered the formation of an AFM planar domain wall in response to the FM magnetization reversal [10]. They showed that the exchange bias in this case depends heavily on the strength of the interfacial coupling and can be classified into two distinct regimes (e.g., $\lambda \ll 1$ regime and $\lambda \gg 1$ regime where λ is the ratio of the FM/AFM interfacial coupling to the AFM planar domain wall energy). In the weak coupling regime ($\lambda \ll 1$), the exchange bias is simply determined by the interfacial coupling as discussed above/previously. In the strong coupling limit ($\lambda \gg 1$), however, the exchange bias does not scale with the FM/AFM interfacial coupling but rather reaches a maximum value corresponding to the formation of a 180° planar domain wall within the AFM. The Mauri's model raises two important questions: (1) Are the AFM bulk spins relevant to the exchange bias? (2) Is the planar domain wall proposed by Mauri responsible for the exchange bias in the strong coupling limit? Early experimental

evidence on Mauri's model was based on indirect observations by measuring the FM hysteresis loops in FM/AFM/FM trilayers [11]. In more detailed experiments combining hysteresis loop and neutron diffraction measurements, however, Steadman et al. showed that neither the AFM domain wall nor the spin flop coupling is related to the exchange bias but that the anisotropy of the antiferromagnet is essential [12]. A clearer demonstration of the bulk AFM spins on the exchange bias was made in a clever designed experiment on Py/FeF₂/Ni trilayer system in which parallel and antiparallel configurations of the Ni and Py magnetizations were obtained through field cooling and were shown to result in distinct exchange bias properties. However, a spring-like domain wall is not expected in the FeF₂ space layer due to its strong uniaxial magnetic anisotropy, i.e. the Mauri planar domain wall model cannot explain the exchange bias in this system [13]. The difficulty in explaining the above described experiments is due to the lack of a direct and element-specific measurement of the AFM spins which became possible only after the development of the X-ray Magnetic Linear Dichroism (XMLD). Only one direct measurement was made so far to confirm the formation of Mauri's AFM planar domain wall. By saturating the Co magnetization on top of a NiO(001) single crystal, the NiO XMLD measurement shows that the Co/NiO interfacial coupling is in the strong coupling regime of Mauri's model ($\lambda=1.53$) and that the NiO spins indeed form a spiral wall as an external magnetic field rotates the Co magnetization by 90° [14]. However, this experiment did not go beyond a 90° spin rotation to verify the existence of the 180° domain wall which is responsible for the exchange bias in the Mauri's model in the strong coupling limit. In addition, their derived domain wall energy yields an exchange bias of ~2 kOe from the Mauri's model which is much larger than the experimental value. Recent experimental results also show inconsistencies between the exchange bias in Py/NiO films and the Mauri model [15]. All these experimental results challenge the Mauri 180° domain wall mechanism for exchange bias in the strong coupling limit. Since many exchange bias theories are based on or related to the Mauri domain wall model [9,16], it is very important to give a firm experimental answer whether a 180° domain wall can exist in the AFM layer during the FM magnetization reversal? In this Letter, we report our experimental study on Fe/NiO/Fe/CoO/Ag(001) using XMCD and XMLD. By pinning the bottom Fe layer magnetization using the CoO layer, we show that the NiO

spins wind up to form a domain wall as the top Fe layer magnetization rotates from 0° to 90° ; but then switch the domain wall chirality to unwind the wall as the top Fe layer magnetization rotates from 90° to 180° . Our result shows that Mauri's 180° domain wall does not exist in perpendicularly coupled FM/AFM system in the strong coupling regime.

A Ag(001) single crystal substrate was cleaned in ultrahigh vacuum by cycles of Ar^+ ion sputtering at $\sim 2\text{keV}$ and annealing at 600°C . $\text{Fe}(10\text{nm})/\text{CoO}(5\text{nm})/\text{Ag}(001)$ films were grown epitaxially on top of the Ag(001) substrate at room temperature. Then half of the sample was covered by a shutter, and on top of the other half of the sample, $\text{Fe}(1.5\text{nm})/\text{NiO}(6\text{nm})$ films were grown to form $\text{Fe}(1.5\text{nm})/\text{NiO}(6\text{nm})/\text{Fe}(10\text{nm})/\text{CoO}(5\text{nm})/\text{Ag}(001)$ films [Fig. 1(a)]. The Fe films were deposited by evaporating Fe at a pressure below 9×10^{-10} Torr, and the CoO and NiO films were grown by evaporating Co and Ni in an oxygen atmosphere of 2×10^{-6} Torr. Fe films on Ag(001) have a bcc structure with the Fe[100] axis parallel to the Ag[110] axis, and CoO and NiO films on Fe(001) or Ag(001) have a rock salt structure with the [110] axis parallel to the Fe[100] axis. The sample is finally covered by a 2-nm Ag-protection layer. Detailed descriptions of sample growth and characterization have been reported previously [17]. Low Energy Electron Diffraction confirms the single crystalline structure of the layers in our sample [Fig. 1(b)]. The sample was measured using X-ray Magnetic Circular Dichroism (XMCD) and X-ray Magnetic Linear Dichroism (XMLD) in total electron yield mode at beamline 4.0.2 of the Advanced Light Source (ALS) of the Lawrence Berkeley National Laboratory.

The sample was cooled down to ~ 90 K from room temperature within a 5000 Oe magnetic field to align the Fe magnetization with the [100] easy magnetization direction [x-axis in Fig. 1(a)]. Since CoO and NiO have the Néel temperature of $\sim 290\text{K}$ and $\sim 520\text{K}$, respectively, field cooling from room temperature should have an effect on the CoO layer only. Previous work on $\text{Fe}/\text{NiO}/\text{Ag}(001)$ indicated that no exchange bias exists for NiO layers thinner than $\sim 6\text{nm}$ after field cooling from the temperature above the NiO Néel temperature [18]. Therefore we do not expect any exchange bias in our system from the Fe/NiO interface after field cooling from room temperature. Our previous work [19] showed that Co spins in CoO films thicker than 2.5nm are strongly coupled to the crystal lattice and induce a strong in-plane uniaxial magnetic anisotropy in the Fe film with the

hard magnetization axis perpendicular to the field cooling direction. We confirmed this result for the Fe(10nm)/CoO(5nm)/Ag(001) sample by measuring Fe hysteresis loops for magnetic fields applied orthogonally to the field cooling direction (H//y-axis). The Fe film exhibits the expected hard axis hysteresis loop with a saturation field of ~ 7000 Oe [red line in Fig. 1(c)]. We also measured the Fe hysteresis loop on the Fe(1.5nm)/NiO(6nm)/Fe(10nm)/CoO(5nm)/Ag(001) sample with the field applied orthogonally to the field cooling direction (H//y-axis). Because of the surface sensitivity of our electron yield measurement, the Fe XMCD signal in this configuration is dominated by the top Fe(1.5nm) layer [blue line in Fig. 1(c)]. In contrast to the Fe(10nm)/CoO(5nm)/Ag(001) hard axis loop, the top Fe(1.5nm) layer in the Fe(1.5nm)/NiO(6nm)/Fe(10nm)/CoO(5nm)/Ag(001) exhibits a square hysteresis loop with a much weaker saturation field of ~ 1500 Oe as compared to the 7000 Oe saturation field of Fe(10nm)/CoO(5nm)/Ag(001). This is understandable taking into account that the magnetic anisotropy of NiO is much weaker as compared to CoO.

By applying a 2000 Oe in-plane magnetic field to align both the top and bottom Fe layer magnetizations of the Fe(1.5nm)/NiO(6nm)/Fe(10nm)/CoO(5nm)/Ag(001) in the field cooling direction, we measured the Ni L_2 edge x-ray absorption spectrum (XAS) for normal incidence of a linearly polarized x-ray beam [Fig. 1(d)]. The Ni XMLD signal R_{L2} (defined as the ratio of the peak intensity occurring at lower photon energy divided by the peak intensity occurring at higher photon energy in the Ni L_2 doublet) exhibits the expected $\cos^2\phi_{x\text{-ray}}$ -dependence on the x-ray polarization angle ($\phi_{x\text{-ray}}$). The R_{L2} value reaches its maximum at $\phi_{x\text{-ray}}=0^\circ$ and minimum at $\phi_{x\text{-ray}}=90^\circ$ [Fig. 1(d)]. Using well-established criteria, the result of Fig. 1(d) shows that the NiO spins are aligned perpendicularly to the Fe magnetizations after field cooling (NiO spins // y-axis), consistent with the reports that the NiO and Fe spins are coupled perpendicularly to each other [20,21]. We then applied an in-plane 2000 Oe magnetic field orthogonal to the field cooling direction (H//y axis). From the result of Fig. 1(c), the 2000 Oe field should align the top Fe(1.5nm) magnetization to the y-axis while the bottom Fe(10nm) magnetization should remain pinned approximately parallel to the x-axis by the CoO. The Fe/NiO interfacial coupling fall in the strong coupling limit since $\lambda=1.53$ for Co/NiO(001) (Ref. 14) which should be similar for Fe/NiO(001). Therefore the Fe/NiO

interfacial coupling at the two Fe/NiO interfaces should twist the NiO spins to form a $\sim 90^\circ$ domain wall with the top NiO spins being rotated from the y-axis to the x-axis and the bottom NiO spins fixed parallel to the y-axis. Indeed the Ni XAS at $\phi_{x\text{-ray}}=0^\circ$ and $\phi_{x\text{-ray}}=90^\circ$ polarizations [Fig. 2(b)] are almost identical under this condition, which is consistent with the NiO 90° domain wall structure since the spin axis ‘averaged’ through the NiO film ($\sim 45^\circ$ to the x-axis) forms an equal angle to the $\phi_{x\text{-ray}}=0^\circ$ and $\phi_{x\text{-ray}}=90^\circ$ polarizations. To further confirm the NiO 90° domain wall structure shown in Fig. 2(b), we applied a 7000 Oe magnetic field orthogonal to the field cooling direction (y-axis) to align both the top and the bottom Fe layer magnetization to the y-axis. Indeed the XAS at $\phi_{x\text{-ray}}=0^\circ$ and $\phi_{x\text{-ray}}=90^\circ$ polarizations [Fig. 2(c)] are interchanged as compared to the result of Fig. 2(a), showing that the NiO spins have been unwound from the 90° domain wall to a single domain with their spins in the x-axis [Fig. 2(c)]. Therefore we conclude that the perpendicular alignment of the two Fe magnetizations twists the NiO spins into a $\sim 90^\circ$ domain wall, consistent with result in Ref. [14] for bulk NiO.

Since an in-plane magnetic field of 2000Oe is sufficient to align the top Fe(1.5nm) layer magnetization parallel to the field direction but weak enough to keep the bottom Fe(10nm) layer magnetization pinned by the CoO, a rotation of the 2000 Oe magnetic field within the film plane is expected to wind the NiO spins continuously inside the NiO film to form a spiral domain wall. We studied this NiO spin winding process by monitoring the Ni XMLD signal as a function of the magnetic field rotation angle (α) at fixed x-ray polarization ($\phi_{x\text{-ray}}=0^\circ$) (Fig. 3). Assuming a rigid perpendicular Fe/NiO interfacial coupling, α is also the rotation angle of the NiO spin axis at the top Fe/NiO interface and the total twisting angle of the NiO spins inside the NiO film. As α increases from 0° to 90° , the Ni XMLD signal $R_{L2}(\alpha)$ decreases monotonically, showing that the NiO spins are indeed wound up to form a spiral domain wall. However, as α increases continuously from 90° to 180° , the Ni XMLD signal $R_{L2}(\alpha)$ is *increasing* instead of decreasing and recovers to its original value at $\alpha=180^\circ$ [i.e., $R_{L2}(0^\circ)\approx R_{L2}(180^\circ)$]. This behavior is opposite to the continuous winding of the NiO spins from a 90° domain wall to a 180° domain wall because such a spin spiral structure should result in a continuous rotation of the averaged NiO spin axis from 45° to 90° , leading to a continuous decrease of the Ni XMLD signal from $\alpha=90^\circ$ to $\alpha=180^\circ$. The fact

that R_{L2} increase from $\alpha=90^\circ$ to $\alpha=180^\circ$ and especially the fact that $R_{L2}(0^\circ)=R_{L2}(180^\circ)$ show that as α increases from 90° to 180° , the NiO spins are actually unwound from the 90° domain wall at $\alpha=90^\circ$ back to a single domain at $\alpha=180^\circ$ with the spins along the y-axis. The reason is that for a perpendicular FM/AFM interfacial coupling there are two types of AFM domain walls: one has a right-handed chirality with the AFM spins winding in the same direction of α to form an α domain wall; the other has a left-handed chirality with the AFM spins winding in the opposite direction of α to form a $180^\circ-\alpha$ domain wall. The right-handed wall has a lower energy than the left-handed wall for $\alpha<90^\circ$ but a higher energy for $\alpha>90^\circ$. Therefore as α increases, the NiO spins initially wind up to form the right-handed domain wall for $\alpha<90^\circ$, then switch the chirality from right-handed to left-handed at $\alpha\sim 90^\circ$, and unwind the left-handed domain wall as α increases from 90° to 180° . Our result shows that for perpendicular FM/AFM interfacial coupling, Mauri's domain wall exists only up to $\sim 90^\circ$ which will generate a uniaxial magnetic anisotropy in the FM film. However, the absence of the 180° domain wall shows that the AFM domain wall cannot produce any exchange bias. Therefore our result rules out the Mauri's exchange bias mechanism for perpendicular FM/AFM coupling. This explains the result of Ref. [12] and why FM/NiO has a much weaker exchange bias than the Mauri's model value [14,18]. Future theoretical models need to find new pinning mechanisms for the exchange bias other than the Mauri's 180° domain wall mechanism.

For a quantitative analysis, we take into account that the probing depth of electron yield detection used in our experiments leads to a contribution of the XMLD signal at a distance z from the NiO surface of $R_{L2}(z) = R_{L2}(0)\exp(-z/\lambda_{NiO})$, where $\lambda_{NiO} = 5.5nm$ is the electron escape depth for NiO [22]. Then the measured XMLD signal is a weighted averaged value of the NiO spin domain wall structure $\langle R_{L2} \rangle = \frac{R_{L2}(0)}{d_{NiO}} \int_0^{d_{NiO}} \cos^2 \phi(z) \exp(-z/\lambda_{NiO}) dz$, where $\phi(z)$ is the NiO twisting angle at position z . Assuming a uniform twist of the NiO spins, we calculated $\langle R_{L2} \rangle$ for a right-handed domain wall [$\phi(z) = \alpha(d_{NiO} - z)/d_{NiO}$] and for a left-handed domain wall [$\phi(z) = (180^\circ - \alpha)(d_{NiO} - z)/d_{NiO}$]. The calculation results shown in Fig. 3 clearly

indicate that the NiO spins undergo a chirality switching at $\alpha \sim 90^\circ$ from the right-handed domain wall in the range of $0^\circ < \alpha < 90^\circ$ to the left-handed domain wall in the range of $90^\circ < \alpha < 180^\circ$. The present experimental accuracy does not allow determining the exact angle at which the chirality switches. It is an interesting topic for future study because such chirality switching involves a topological change of the domain wall structure. We should mention that in our calculation we have assumed that the bottom Fe magnetization is fixed in the x direction whereas in fact the 2000 Oe field should rotate the bottom Fe magnetization slightly away from the x direction. With the 7000 Oe saturation field in Fig. 1 for Fe/CoO/Ag(001), we estimate that the bottom Fe magnetization should rotate by $\sim 15^\circ$ away from the x-axis for a 2000 Oe field applied in the y-axis. This effect would reduce the $\langle R_{L2} \rangle$ value only by $\sim 6\%$ at $\alpha = 90^\circ$ because the exponential factor of $\exp(-z/\lambda_{\text{NiO}})$ in $\langle R_{L2} \rangle$ makes the XMLD contribution from the bottom NiO much weaker than from the top NiO.

In summary, we performed element-specific XMCD and XMLD measurement on Fe/NiO/Fe/CoO/Ag(001) films. By pinning the bottom Fe magnetization with the CoO layer and rotating the top Fe magnetization with an in-plane magnetic field, we measured the NiO spiral spin structure and domain wall formation. We show that as the top Fe magnetization rotation angle (α) increases, the NiO spins wind up to form a right-handed domain wall from $\alpha = 0^\circ$ to $\alpha = 90^\circ$, then switch the domain wall chirality from right- to left-handed at $\alpha \sim 90^\circ$, and unwind the left-handed domain wall from $\alpha = 90^\circ$ to $\alpha = 180^\circ$. The absence of the 180° domain wall shows that Mauri's planar domain wall mechanism cannot be applied to the exchange bias in the strong coupling limit for perpendicular ferromagnetic/antiferromagnetic interfacial coupling. The existence of the 90° domain wall allows Mauri's model to induce a uniaxial magnetic anisotropy in the FM layer.

Acknowledgement

This work was supported by National Science Foundation DMR-0803305, U.S. Department of Energy DE-AC02-05CH11231, National Science Foundation of China, ICQS of Chinese Academy of Science, and KICOS through Global Research Laboratory project.

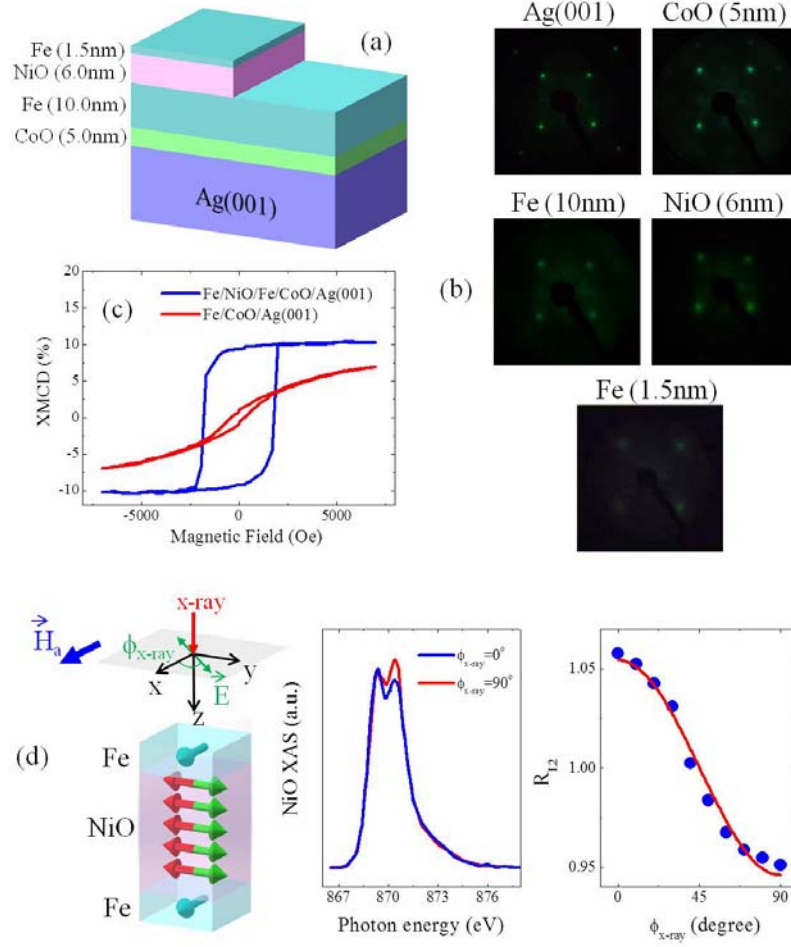


Fig. 1: (Color online) (a) Schematic drawing of the Fe/CoO and the Fe/NiO/Fe/CoO samples grown on top of the same Ag(001) substrate. (b) LEED patterns confirm the epitaxial growth of Fe(1.5nm)/NiO/Fe(10nm)/CoO/Ag(001) films. (c) For field applied orthogonal to the field cooling direction, the Fe/CoO/Ag(001) sample exhibits a hard-axis hysteresis loop (red line) because of the CoO pinning effect but the top Fe layer in Fe/NiO/Fe/CoO/Ag(001) exhibits a square shape hysteresis loop because of the soft AFM NiO layer. (d) With a 2000 Oe external field applied in the field cooling direction, the Ni L2 edge exhibits the expected XMLD effect as indicated by the $\cos^2 \phi_{x-ray}$ -dependence of the L_2 ratio R_{L2} .

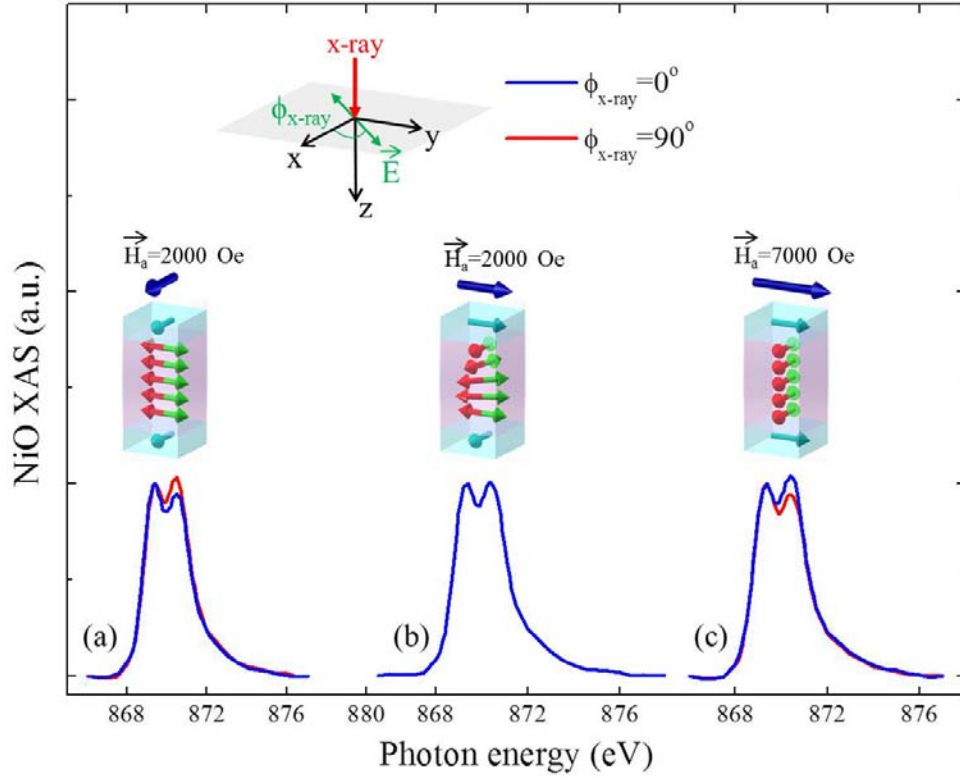


Fig. 2: (Color online) Ni XAS of the Fe/NiO/Fe/CoO/Ag(001) sample at two polarizations of the x-rays. (a) When a 2000 Oe magnetic field is applied in the field cooling direction, the NiO spins form a single domain with the spins parallel to the y-axis. (b) When a 2000 Oe magnetic field is applied orthogonal to the field cooling direction, the top Fe layer magnetization switches from x direction to y direction to wind the NiO spins into a 90° domain wall, resulting in an identical Ni XAS for the two x-ray polarizations. (c) When a 7000 Oe magnetic field is applied orthogonal to the field cooling direction, both the top and bottom Fe layer magnetizations switch from x direction to y direction to unwind the NiO 90° domain wall into a single domain with the spins parallel to the x-axis, resulting in a switching of the Ni XAS as compared to (a).

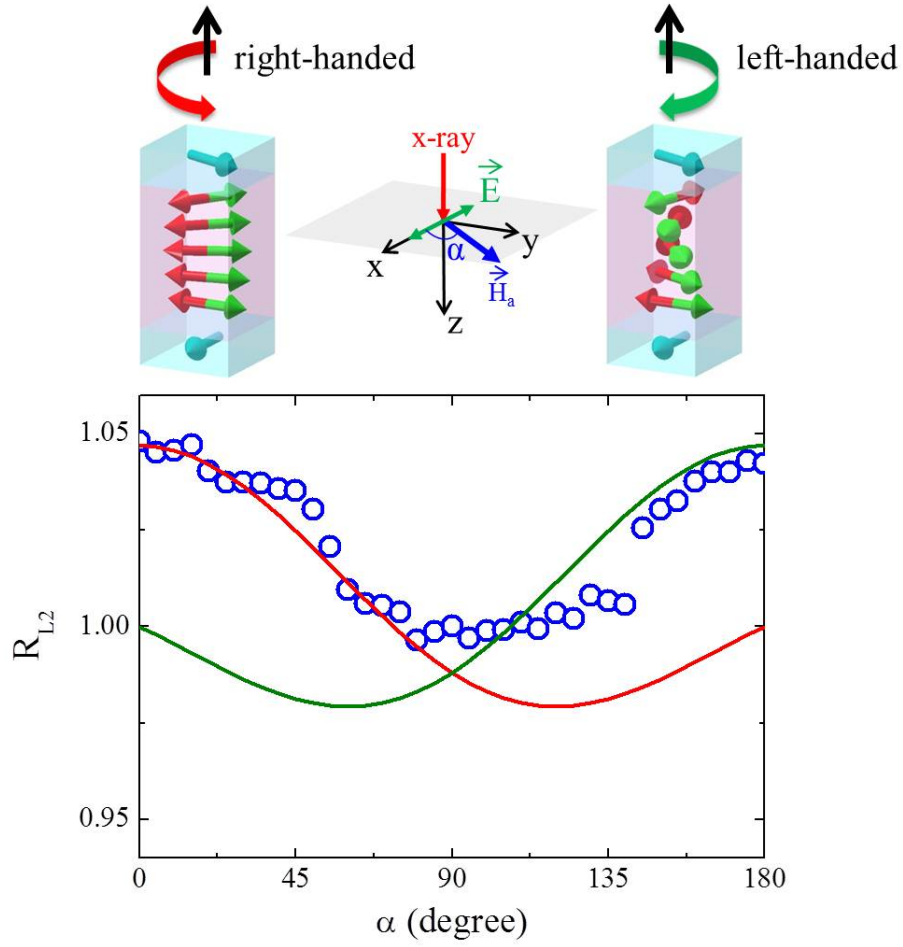


Fig. 3: (Color online) As top Fe layer magnetization is rotated (rotation angle α) by a 2000 Oe magnetic field, the NiO spins wind up to form a domain wall $0^\circ < \alpha < 90^\circ$, switch the wall chirality at $\alpha \sim 90^\circ$, and unwind for $90^\circ < \alpha < 180^\circ$. The red and green lines are calculated XMLD results for right-handed and left-handed NiO domain walls, respectively.

References:

1. W. H. Meiklejohn and C. P. Bean, Phys. Rev. **102**, 1413 (1956).
2. J. Nogués and Ivan K. Schuller, J. Magn. Magn. Mater. **192**, 203 (1999).
3. W. H. Meiklejohn, J. Appl. Phys., **33** 1328 (1962).
4. A. P. Malozemoff, Phys. Rev. B **35**, 3679 (1987).
5. N.C. Koon, Phys. Rev. Lett. **78**, 4865 (1997).
6. T. C. Schulthess and W. H. Butler, Phys. Rev. Lett. **81**, 4516 (1998).
7. M. D. Stiles and R. D. McMichael, Phys. Rev. B **59**, 3722 (1999).
8. P. Miltényi, M. Gierlings, J. Keller, B. Beschoten, and G. Güntherodt, U. Nowak, and K. D. Usadel, Phys. Rev. Lett. **84**, 4224 (2000).
9. Miguel Kiwi, J. Magn. Magn. Mater. **234**, 584 (2001).
10. D. Mauri, H. C. Siegmann, P. S. Bagus, and E. Kay, J. of Appl. Phys. **62**, 3047 (1987).
11. F.Y. Yang and C. L. Chien, Phys. Rev. Lett. **85**, 2597 (2000).
12. P. Steadman, M. Ali, A. T. Hindmarch, C. H. Marrows, B. J. Hickey, Sean Langridge, R. M. Dalgliesh, and S. Foster, Phys. Rev. Lett. **89**, 077201 (2002).
13. R. Morales, Zhi-Pan Li, J. Olamit, Kai Liu, J. M. Alameda, and Ivan K. Schuller, Phys. Rev. Lett. **102**, 097201 (2009).
14. A. Scholl, M. Liberati, E. Arenholz, H. Ohldag, and J. Stöhr, Phys. Rev. Lett. **92**, 247201 (2004).
15. J. McCord and S. Mangin, Phys. Rev. B **88**, 014416 (2013).
16. J. Moritz, P. Bacher, and B. Dieny, Phys. Rev. Lett. **112**, 087201 (2014).
17. J. Wu, J. S. Park, W. Kim, E. Arenholz, M. Liberati, A. Scholl, Y. Z. Wu, Chanyong Hwang, and Z. Q. Qiu, Phys. Rev. Lett. **104**, 217204 (2010).
18. P. Luches, S. Benedetti, A. di Bona, and S. Valeri, Phys. Rev. B **81**, 054431 (2010).
19. J. Li, Y. Meng, J. S. Park, C.A. Jenkins, E. Arenholz, A. Scholl, A. Tan, H. Son, H. W. Zhao, Chanyong Hwang, Y. Z. Wu, and Z. Q. Qiu, Phys. Rev. B **84**, 094447 (2011).
20. M. Finazzi, M. Portalupi, A. Brambilla, L. Duò, G. Ghiringhelli, F. Parmigiani, M. Zacchigna, M. Zangrando, and F. Ciccacci, Phys. Rev. B **69**, 014410 (2004).
21. J. Wu, D. Carlton, J. S. Park, Y. Meng, E. Arenholz, A. Doran, A.T. Young, A. Scholl, C. Hwang, H. W. Zhao, J. Bokor, and Z. Q. Qiu, Nature Physics **7**, 303-306 (2011).
22. Y. Z. Wu, Y. Zhao, E. Arenholz, A. T. Young, B. Sinkovic, C. Won, and Z. Q. Qiu, Phys. Rev. B **78**, 064413 (2008).